Available online at www.sciencedirect.com

Journal of Photochemistry and Photobiology A: Chemistry 174 (2005) 214–221

Journal of Photochemistry and Photobiology A:Chemistry

www.elsevier.com/locate/jphotochem

Photoactivity and photoselectivity of a dielectric metal-oxide photocatalyst (ZrO_2) probed by the photoinduced reduction of oxygen and oxidation of hydrogen

A.V. Emeline[a,1], G.N. Kuzmin[b], L.L. Basov[b], N. Serpone[c,*]

[a] Kanagawa Academy of Science and Technology, KSP West 614, 3-2-1 Sakado, Takatsu-ku, Kawasaki-shi, Kanagawa 213-0012, Japan
[b] Department of Photonics, Institute of Physics, State University of St. Petersburg, St. Petersburg, Russia
[c] Dipartimento di Chimica Organica, Università di Pavia, Via Taramelli 10, Pavia 27100, Italy

Received 23 December 2004; received in revised form 13 March 2005; accepted 17 March 2005
Available online 25 April 2005

Abstract

The photoinduced reduction of oxygen and photooxidation of hydrogen occurring on *oxidized* and *reduced* surfaces of the metal-oxide dielectric material ZrO_2 (in monoclinic form) have been examined to probe the spectral variations of the photoactivity and photoselectivity of this metal oxide by determining (true) photochemically defined quantum yields for the two redox reactions at various wavelengths of photoexcitation ($200\,\text{nm} < \lambda < 400\,\text{nm}$). Irradiation of zirconia in the fundamental absorption (*intrinsic*; $\lambda < 260\,\text{nm}$) region leads predominantly to the photoreduction of oxygen, whereas the photooxidation of hydrogen predominates on irradiation in the *extrinsic* spectral region ($260\,\text{nm} < \lambda < 360\,\text{nm}$). A pathway for the formation of electron-trapped states (Zr^{3+}) and hole-trapped states ($O^{\bullet -}$) in the extrinsic spectral region is described since both oxidation and reduction take place in this extrinsic region with oxidation predominating. The reported experimental results provide the long sought-after spectral variations into the photoactivity and photoselectivity of metal-oxide photocatalysts in gas/solid heterogeneous systems.

© 2005 Elsevier B.V. All rights reserved.

Keywords: Photoactivity; Photoselectivity; Zirconia; Dielectric metal oxide; Photoinduced reduction of oxygen; Photoinduced oxidation of hydrogen; Oxidized ZrO_2 surface; Reduced ZrO_2 surface; Color centers; Surface defects; Quantum yields

1. Introduction

Improving the activity and selectivity of photocatalysts is a major challenge in studies of photochemical processes taking place in heterogeneous systems. To meet this challenge, a better understanding of the key-factors that govern their activity and selectivity is of great importance in heterogeneous photocatalysis, which describes the generalization of a chemical reaction that converts reagent M molecules to product P molecules $\{\text{i.e. } M \rightarrow P\}$, a heterogeneous catalytic reaction $\{M + \text{Cat} \rightarrow P + \text{Cat}\}$, and a photochemical reaction $\{M + \text{light} \rightarrow P\}$ with involvement of free energy in the process. When the catalytic cycle is incomplete (i.e. Cat is not restored), the process then represents a simple stoichiometric heterogeneous photoreaction. Examples of such photoreactions are the photoadsorption of molecules when the reaction product is strongly bonded to the surface of the solid [1–7]. Typically, the initial steps of photoexcitation of heterogeneous systems are the same for both photocatalytic and non-photocatalytic chemical processes, regardless of the final result of secondary surface chemical reactions. The photoadsorption step is often the first chemical event in heterogeneous photocatalysis.

There are several different photochemical processes that can occur in heterogeneous systems and which are distinguished only by their mechanistic behavior [8–10]. The major pathway involves first the photogeneration of free charge

---

* Corresponding author. Tel.: +39 0382 98 78 35; fax: +39 0382 98 73 23.
E-mail addresses: nick.serpone@unipv.it, serpone@vax2.concordia.ca (N. Serpone).

[1] Previous address: Concordia University, Montreal, Canada.

1010-6030/$ – see front matter © 2005 Elsevier B.V. All rights reserved.
doi:10.1016/j.jphotochem.2005.03.011

carriers (electrons, e^-; holes, h^+) in the solid photocatalyst that are subsequently localized on the surface poised to interact with molecules (M) to initiate chemical changes that ultimately yield reaction products P1 and P2 (Eqs. (1) and (2)):

$$\mathrm{M} + \mathrm{e_S}^- \rightarrow \mathrm{M}^- \rightarrow \mathrm{P1} \quad k_\mathrm{e} \tag{1}$$

$$\mathrm{M} + \mathrm{h_S}^+ \rightarrow \mathrm{M}^+ \rightarrow \mathrm{P2} \quad k_\mathrm{h} \tag{2}$$

The activity of the metal-oxide photocatalyst can be characterized by the quantum yield (Φ) of photoreaction in the heterogeneous system, with Φ defined precisely as is done in homogeneous photochemistry [11]—Eq. (3):

$$\Phi = \frac{\mathrm{d}N_\mathrm{M}/\mathrm{d}t}{\mathrm{d}N_{h\nu}/\mathrm{d}t} = \frac{(k_\mathrm{e}[\mathrm{e}^-] + k_\mathrm{h}[\mathrm{h}^+])[\mathrm{M}]}{f\rho} \tag{3}$$

where N_M is the number of M molecules being reduced and/or oxidized, $N_{h\nu}$ is the number of photons absorbed, f is the fraction of photons absorbed by the heterogeneous system and ρ is the photon flow of the incident actinic light. Eq. (3) also shows that the photoactivity of a metal-oxide catalyst is determined by the surface concentrations of the charge carriers (e^- and h^+) and by the corresponding reaction rate constants k_e and k_h (Eqs. (1) and (2)). In turn, both $[\mathrm{e}^-]$ and $[\mathrm{h}^+]$ depend strongly on the spatial distribution of photogeneration of carriers, and on their lifetimes and mobilities [12,13]. Combination of these factors results in the spectral variation of the surface concentrations of charge carriers, and thus the activity of photocatalysts depends on the spectral variation of the absorption coefficient of the solid. In turn, the lifetimes of the charge carriers are strongly dictated by the efficiency of charge carrier trapping by and recombination through defects in the solid. In a simplified presentation, the lifetime of a charge carrier (τ) is given by $\tau = 1/\sum_i k_i N_i$, where N_i is the number of ith-sort carrier traps, and k_i is the corresponding rate constant of carrier trapping. Thus, the higher is the concentration of the corresponding defects in the solids and the higher is the efficiency of carrier trapping and recombination, the shorter will be the lifetime of free charge carriers and the lower will be their concentration on the surface. Thus, the activity of a photocatalyst is dictated by the efficiency of bulk and surface electronic processes, both of which lead to the spectral dependence of the activity of photocatalysts.

Another major feature of the metal-oxide solid in a heterogeneous system is the selectivity of the photocatalyst toward certain products (S_i) given by the ratio of the rate of formation of a given product R_i to the sum of rates of formation of all reaction products (or rate of consumption of the reagents), $\sum_i R_i$, in the heterogeneous photoreaction: that is, $S_i = R_i/\sum_i R_i$. In a simple interfacial photochemical reaction, the selectivity of the photocatalyst toward either P1 or P2 is then given by Eqs. (4) and (5), respectively:

$$S_\mathrm{P1} = \frac{k_\mathrm{e}[\mathrm{e}^-]}{k_\mathrm{e}[\mathrm{e}^-] + k_\mathrm{h}[\mathrm{h}^+]} = \frac{(k_\mathrm{e}/k_\mathrm{h})\gamma}{(k_\mathrm{e}/k_\mathrm{h})\gamma + 1} \tag{4}$$

$$S_\mathrm{P2} = \frac{k_\mathrm{h}[\mathrm{h}^+]}{k_\mathrm{e}[\mathrm{e}^-] + k_\mathrm{h}[\mathrm{h}^+]} = \frac{1}{(k_\mathrm{e}/k_\mathrm{h})\gamma + 1} \tag{5}$$

where $\gamma = [\mathrm{e}^-]/[\mathrm{h}^+]$ is the ratio of the concentrations of carriers on the photocatalyst surface. Consequently, the selectivity depends on γ and on the ratio of rate constants for the reductive (k_e) and oxidative (k_h) reactions. The reductive pathway predominates when $(k_\mathrm{e}/k_\mathrm{h})\gamma \gg 1$, that is, when either $k_\mathrm{e} \gg k_\mathrm{h}$ or $[\mathrm{e}^-] \gg [\mathrm{h}^+]$. For the opposite case, the oxidation pathway predominates. Accordingly, the spectral variation of $[\mathrm{e}^-]/[\mathrm{h}^+]$ causes the spectral variation of the selectivity of a photocatalyst [12–14].

As noted earlier, the initial steps of photoprocesses in heterogeneous systems are common regardless of the type of photoreactions. Accordingly, such a simple photoreaction as the photoinduced surface redox reactions of such probe molecules as O_2 and H_2 should reflect the major

$$\mathrm{e}^- + \mathrm{S_e} \rightarrow \mathrm{S_e}^- \xrightarrow{\mathrm{O_2}} \mathrm{O_{2\,ads}}^{\bullet -} \tag{6}$$

$$\mathrm{h}^+ + \mathrm{S_h} \rightarrow \mathrm{S_h}^+ \xrightarrow{\mathrm{H_2}} \{\mathrm{H_{2\,ads}}\} \rightarrow \{\mathrm{H}^+ + \mathrm{H}^\bullet\} \tag{7}$$

features of a photocatalyst, particularly the spectral variation of surface concentrations of electrons and holes and their ratio γ, and as result the spectral variation of the activity and selectivity of the photocatalyst. In Eqs. (6) and (7), S_e and S_h denote the surface-active centers of photoreduction of oxygen and photooxidation of hydrogen.

In the present article we report experimental data that demonstrate the spectral dependence of quantum yields of the photoinduced reduction of oxygen as a probe for surface electrons, and the photooxidation of hydrogen as a probe for surface holes on zirconia particles. Moreover, we delineate the spectral regions in which photoreduction of oxygen and photooxidation of hydrogen predominate for *oxidized* and reduced zirconia specimens.

2. Experimental

The powdered monoclinic form of the ZrO_2 specimens produced from zirconium(IV) oxychloride was of high purity grade (“7–4”, IREA, Russia). The specific surface area of the sample determined by the BET method with nitrogen gas was ca. 7 $m^2\,g^{-1}$. Adsorbed water and organic impurities were removed from the surface of the metal-oxide specimens by prior treatment at 900 K in an oxygen atmosphere ($p \approx 100$ Pa) for several days. Before every measurement, samples were preheated in an O_2 atmosphere at 900 K for 30 min and then cooled under dynamic vacuum. X-ray diffraction structural methods (X-ray diffractometer DRON-2, Co KR line) confirmed that high-temperature pretreatment and pre-irradiation of the zirconia samples caused no modifications to the crystal form. Experimental errors in the measurements caused by the reproducibility of the original state of the specimen do not exceed ca. 15%.

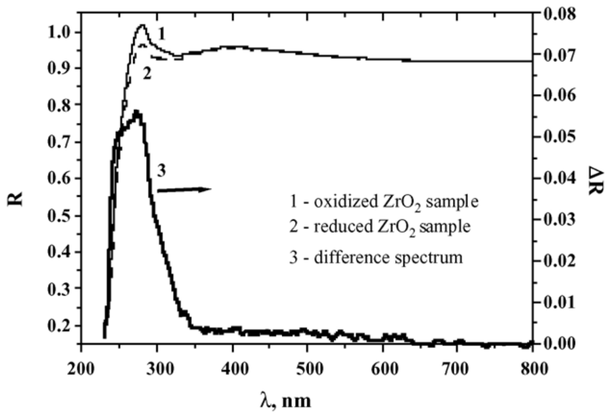

Fig. 1. Graph displaying the diffuse reflectance spectra (R) of the oxidized ZrO_2 specimen (spectrum 1) and the reduced zirconia sample (spectrum 2). Spectrum 3 illustrates the difference diffuse reflectance spectrum (as ΔR) of the defect centers obtained as (spectrum 1) minus (spectrum 2) – note that the ΔR spectrum is equivalent to the change-in-absorption ΔA spectrum of the defect centers in the extrinsic wavelength region ca. 240–350 nm. Note that the error in R does not exceed 0.001 in absolute values.

Samples were contained in quartz “blackbody”-like cells specially designed by Basov and Solonitsyn [15] to measure quantum yields of heterogeneous photoreactions; details of the procedure were given in an earlier article [16]. Oxidized and reduced zirconia specimens were obtained by a procedure also reported earlier [1]. In essence, the oxidized state of the zirconia surface was formed by pre-heating the sample at 600 °C in an oxygen atmosphere inside the cell. By contrast, the reduced state of the ZrO_2 surface was produced by pre-heating the sample inside the cell in a hydrogen atmosphere for 1 h followed by continued heating under dynamic vacuum at 600 °C for 10 h. Fig. 1 shows the corresponding diffuse reflectance spectra of the oxidized (spectrum 1) and reduced (spectrum 2) ZrO_2 samples, together with the absorption spectrum (3) of defect centers. The mass of the sample in the blackbody-like cells was such (ca. 1 g) as to prevent light transmittance through the external wall, and thus ensuring that complete light absorption by the ZrO_2 specimen occurred in the black-body like cells. The major advantage of the type of cell design used [15] is that there is no need to carry out spectroscopic measurements, since the absorptance (i.e. fraction of light absorbed [11]) of the incident light of any wavelength that penetrates through the small inlet is unity, even for very weak absorption by the metal-oxide specimen.

The reaction cell was connected to a high-vacuum setup equipped with an oil-free pump system; residual pressure in the cell was ca. 10^{-7} Pa. A modified Pirani-type manometer with sensitivity $35\,\mathrm{mV\,Pa^{-1}}$ for O_2 and $42\,\mathrm{mV\,Pa^{-1}}$ for H_2 was used to measure gas pressure in the reactor. The illuminating system was a 120 W xenon lamp DKSH-120 (MELZ) with a monochromator MSD-1 (LOMO) for wavelength selection. The spectral resolution was ca. 5 nm. The incident light irradiance was determined using a thermoelement $\{$IOFI; sensitivity, $20\,\mathrm{mV\,W^{-1}}\}$. Suitable cutoff glass filters (LOMO) eliminated any detrimental scattered light behind the output slit of the monochromator. Metal-supported neutral quartz filters (Vavilov SOI) were used to vary the intensity of the actinic light.

3. Results and discussion

Zirconium dioxide, ZrO_2, finds many useful applications among which are: (1) as a component in super-fine particle films on light permeable plates for image display panels [17]; (2) in microfiltration membranes [18]; (3) as a humidity sensing porous material [19], (3) as a catalyst and catalyst support [20]; (4) when stabilized by added metal oxides (e.g. CaO, Y_2O_3), as a solid electrolyte to measure the oxygen activity in steel making [21]; (5) as a component in all-ceramic fixed partial dentures [22]; (6) as a component in combustible-gas-sensitive gas-symmetric electrolytic cells with oxide-ion-conducting solid electrolytes [23]; (7) in magnetic storage media [24]. Moreover, zirconia belongs to the class of photoresistant metal oxides, and typical of this class new defect centers are formed by trapping of carriers by existing lattice defects [25].

The principal intrinsic defects in powdered zirconia are anion vacancies, V_a [26]. UV irradiation of this dielectric gives rise to broad absorptions in the 250–900 nm spectral region assigned to formation of electron (Zr^{3+}, F and F^+ species) and hole (V-like) color centers [27,28]. Trapping of photoelectrons by the positively charged anion vacancy sites (V_a) generates F^+ and F centers in the zirconia lattice. The presence of Zr^{4+} defect sites (particularly reasonable at irregular near-surface sites) rationalizes the photogeneration of Zr^{3+} centers by electron capture. The existence of such defect Zr^{4+} cations with coordination other than regular Zr^{4+} cations has been treated in some detail in the work by Harrison et al. [29]. For instance, these authors treated the 280–300 nm luminescence band in ZrO_2 as originating from the reaction: $Zr^{5+} + e^- \rightarrow (Zr^{4+})^* \rightarrow Zr^{4+} + h\nu$, in a manner such that the Zr^{4+} cations serve as centers for hole capture. However, the nature of the luminescence was disputed by Bettinali and coworkers [30,31] and by others [27,32]. Whatever the nature of the 280–300 nm emission, the crystallographic work of Harrison et al. [29] supports the notion of preexisting Zr^{4+} defect sites in zirconia, in accord with the mechanism of defect formation via photocarrier trapping by preexisting lattice defects.

The nature of photogenerated hole centers in zirconia is less certain. Intrinsic and extrinsic preexisting hole traps no doubt exist with Harrison’s [29] Zr^{4+} being among them. The trapped hole O^--like center ($g_1 = 2.0196$, $g_2 = 2.101$, and $g_3 = 2.0045$) was detected by Burukina [33] and Prudnikov [34] by EPR techniques both at the surface and in the bulk of the zirconia lattice after UV irradiation by a mercury lamp (note the same ZrO_2 sample and same irradiation source were used as in the present study). The growth kinetics of O^- centers under illumination correlate with the growth kinetics of the color centers detected by diffuse reflectance spectra; the surface O^- trapped holes vanish upon post-illumination adsorption of H_2. Similar EPR signals of these O^- hole centers were reported for γ-irradiated zirconia [35]. Mechanistic details of defect formation in ZrO_2 under a variety of experimental conditions have been reported in several studies [36–46].

3.1. Photoactivity

Zirconia (ZrO_2; $E_{bg} \sim 5.0$ eV) is an active and typical photoadsorbent and photocatalyst among wide band gap metal oxides in accordance with the empirical correlations between the metal oxide's photoinduced adsorption (PhA) activity and its band-gap energy E_{bg}. [47]. The fundamental absorption edge of this metal oxide is ca. 250 nm (intrinsic absorption occurs at wavelengths below 250 nm). The red limit of the PhA for O_2, H_2, CH_4, and C_2H_6 on powdered ZrO_2 [37,43,48] occurs at approximately 3.0 eV ($\lambda = 410$ nm) in the extrinsic absorption band region. The PhA of methane and ethane is the first stage of their photooxidation and conversion to other hydrocarbons [43,49]. The quantum yield Φ of photooxidation of propene, for example, over powdered zirconia is ~0.03 [50], whereas Φ of PhA of O_2 reaches 0.02 on irradiation at the red edge of the fundamental absorption band [51]. ZrO_2 powder is photocolored under UV excitation due to formation of stable defects (color centers). The color centers localized at the surface serve as long-lived PhA centers (i.e. as post-irradiation adsorption centers) for acceptor (O_2) and donor (H_2, CH_4) molecules, respectively. The activity of the PhA centers for O_2 under UV illumination of ZrO_2 (~90%) had earlier been assigned to shallow trap centers whose lifetimes τ ranged from 10^{-2} to 10^{-3} s [42,52]. More recent studies [53,54], however, have demonstrated that short-lived active centers in ZrO_2 are the same as the long-lived centers of post-irradiation adsorption. Differences in lifetimes are dictated by recombination of carriers through these surface defects during irradiation (thus short-lived sites), but when irradiation is terminated these same sites become the long-lived sites for post-irradiation adsorption.

In a set of preliminary experiments, we established that the chosen experimental conditions ($P_{gas} = 3$ Pa) satisfied two major requirements for determining quantum yields: (i) the rate of the photoprocess was maximal at the saturation level in the dependence of rate on gas pressure, and (ii) the dependence of the rate of the photoprocess scaled linearly with light irradiance [53]. These two conditions stipulate that the rate of a photoprocess, and therefore its quantum yield, reflects the maximal efficiency of the photogeneration of reactive sites on the surface of the photocatalyst.

Figs. 2 and 3 illustrate, respectively, the experimental spectral variations of quantum yields of the photoinduced reduction of oxygen and oxidation of hydrogen on oxidized and reduced zirconia surfaces. In both cases, the spectral region of photoactivity of zirconia can be divided into two parts: (i) a spectral region corresponding to intrinsic fundamental absorption ($\lambda < 260$ nm) caused by band-to-band electron transitions, and (ii) a spectral region corresponding to extrinsic light absorption by defects and surface states in the 260–400 nm region.

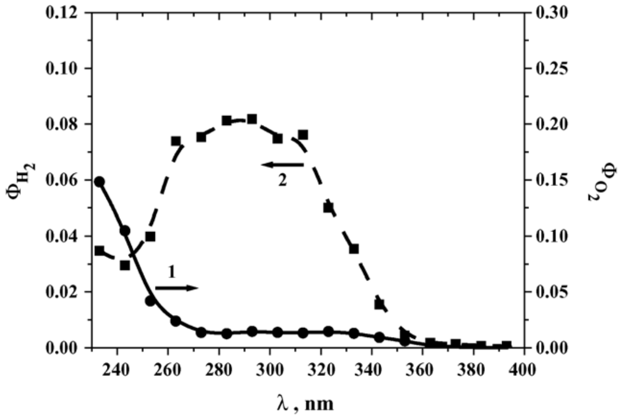

Fig. 2. Spectrally dependent quantum yields for the photoinduced reduction of oxygen (1) and the photoinduced oxidation of hydrogen (2) on oxidized zirconia particles.

Earlier theoretical modeling and expectations [12,13] indicate that the quantum yield of a photochemical process remains constant within a single absorption band for weak extrinsic light absorption, regardless of whether the surface or the bulk of the metal oxide absorbs the incident radiation. However, when a background of inactive absorption (or active absorption with less efficiency for charge separation) overlaps with active absorption, the spectral dependence of the quantum yield can be transformed into a band-like or a step-like shape [12,16]. In this case, the expression for the quantum yield is given by Eq. (8):

$$\Phi_{obs} = \frac{\alpha_a \Phi_a}{\alpha_a + \alpha_{in}} \tag{8}$$

where α_a and α_{in} are the absorption coefficients of the active and inactive absorption bands, respectively, Φ_a the quantum yield of the photoprocess with respect to the active absorption

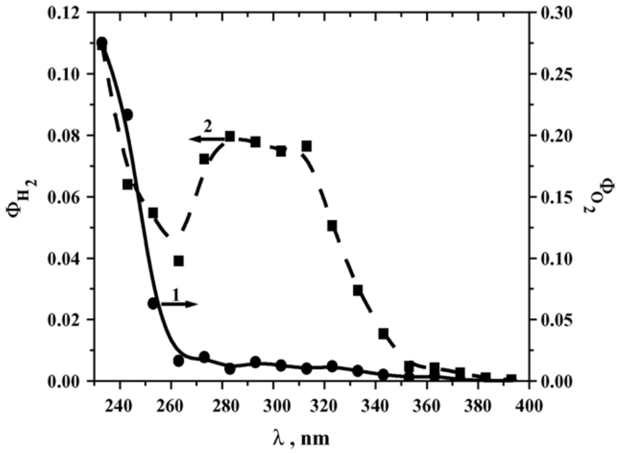

Fig. 3. Spectrally dependent quantum yields for the photoinduced reduction of oxygen (1) and the photoinduced oxidation of hydrogen (2) on reduced zirconia particles.

only, and Φ_{obs} is the experimentally observed quantum yield. From Eq. (8), Φ increases with increase of active absorption, and is constant when $\alpha_a \gg \alpha_{in}$. This conclusion corresponds to the experimentally observed spectral dependencies of photoinduced reactions of both O_2 and H_2 in the spectral region of extrinsic light absorption. The remarkable feature of extrinsic photoexcitation of zirconia is that it leads to both oxidation (photoadsorption of H_2) and reduction (photoadsorption of O_2) at specific surface sites yielding surface type complexes. This behavior is important in terms of photocatalysis which requires that both reactions complete the catalytic cycle. This implies that photogeneration of electrons and holes also occurs during extrinsic photoexcitation of the metal oxide. For instance, Moon et al. [55,56] have suggested that photoexcitation of low-coordinated (LC) ZrO_2 surface sites may be responsible for this behavior. Indeed, a photoinduced charge transfer process in such surface-type complexes results in charge separation to yield electron-donor (Zr^{3+}) and electron-acceptor ($O^{\bullet -}$) surface states (Eq. (9)):

$$(Zr^{4+} - O^{2-})_{LC} + h\nu \rightarrow (Zr^{3+} - O^{\bullet -})^*_{LC} \quad (9)$$

Absorption in the extrinsic spectral region can also be attributed to light absorption by Zr^{3+} defects formed through electron trapping by low-coordinated Zr^{4+} sites. These defects can be produced by thermoreduction of zirconia as evidenced by the appearance of ESR Zr^{3+} signals [57,58] and by absorption bands in UV–vis diffuse reflectance spectra [1,37].

Photoexcitation of such defects leads to photoionization (Eq. (10)) producing free charge carriers, in this case free electrons. However, this pathway does not explain the

$$Zr^{3+} + h\nu \rightarrow Zr^{4+} + e^- \quad (10)$$

concomitant photoinduced formation of hole states for the photooxidation of hydrogen in the same extrinsic spectral region. Applied to this type of defects, the center conversion model [59,60] indicates that hole states can also form considering that Zr^{3+} ions are in low-coordinated positions (Eqs. (11a)–(11c)) which cause strong local distortion in the nearest neighborhood of an otherwise periodic potential:

$$(Zr^{3+} - O^{2-})_{LC} + h\nu \rightarrow (Zr^{4+} - O^{2-})_{LC}{}^* + e^- \quad (11a)$$

$$(Zr^{4+} - O^{2-})^*_{LC} \rightarrow (Zr^{3+} - O^{\bullet -})^*_{LC} \quad (11b)$$

$$(Zr^{3+} - O^{\bullet -})^*_{LC} \rightarrow (Zr^{3+} - O^{2-})_{LC} + h^+ \quad (11c)$$

Thus, the precise mechanism of photoexcitation in the extrinsic spectral region remains somewhat uncertain.

Another feature evident from the experimental data is that surface reduction does not change the values and the spectral dependence of the quantum yields of photoreactions of both oxygen and hydrogen. This can easily be explained within the model of photoexcitation of surface states (Eq. (9)). Even if the number of corresponding surface states were to change by surface reduction, by definition the quantum yield should remain the same provided that excited states remain localized on (or very close to) the surface without exchange of excitation with the bulk. This leads to a so-called *isolated surface*. However, the quantum yield of photoreduction of oxygen is much less than the quantum yield of photooxidation of hydrogen, which infers the possible existence of an electron sink in the bulk of zirconia particles. At the same time, if such an electron sink does exist, its efficiency at trapping electrons is not affected by reduction of the surface.

The photoexcitation model described by Eqs. (11a)–(11c) can also provide an interpretation of the spectral variation of quantum yields and their independence on the (reduced or oxidized) state of the surface. On the one hand, the values of Φ do not depend on the state of the surface if reduction or oxidation of the metal-oxide surface does not significantly affect the surface potential and the sub-surface electric field. In this case, any difference between quantum yields of photoprocesses that involve electrons and holes is dictated by differences in mobilities and lifetimes of the different charge carriers [12,13], provided that surface reduction does not cause significant changes in such properties of charge carriers. On the other hand, if surface reduction does change the surface potential and the sub-surface electric field, Φ would then remain the same only if the Zr^{3+}defects are localized at the surface or are very close to the surface [13]; see also Refs. [57,61–64] for the characterization of surface Zr^{3+} centers. This means that the depth of the space charge region of their localization is smaller than the Debye screening length, and therefore the potential gradient within this region is small, which is the condition for the vanishing influence of the electric field on charge carrier transport to the surface.

The spectral region at wavelengths below 260 nm corresponds to the fundamental bulk absorption of zirconia (intrinsic excitation). According to the models examined earlier by Emeline et al. [12,13], a strong variation of the absorption coefficient at the fundamental absorption edge strongly affects the spatial distribution of photogeneration of charge carriers in the bulk of the photocatalyst that cuddles the space of photogeneration at the surface for higher values of the absorption coefficient, thus increasing the surface concentration of charge carriers. The latter results in an increase of the quantum yield of the photoprocess with an increase of the absorption coefficient at the edge of the fundamental absorption. Clearly, the experimental dependencies of Φ of photoinduced reduction and oxidation of O_2 and H_2, respectively, at the fundamental absorption edge of zirconia (i.e. at $\lambda < 260$ nm) behave according to model predictions; that is, the quantum yields of both photoreactions increase toward shorter wavelengths [12,13].

The surface transformation from oxidized to reduced states causes remarkable changes in the values of the quantum yields of photoreactions of both oxygen and hydrogen in the spectral region of fundamental absorption. Moreover, surface reduction leads to a significant increase in the efficiency of both photoreactions (ca. 30% for hydrogen oxidation, and 100% for oxygen reduction; compare Fig. 2 with Fig. 3). This effect can be explained by changes in the lifetimes of charge carriers caused by surface reduction. Indeed, surface reduction causes formation of Zr^{3+} states at the surface and therefore decreases the number of electron traps (Zr^{4+}), which in turn leads to longer lifetimes for free electrons and increases the probability for electrons photogenerated in the bulk to reach the surface. At the same time, Zr^{3+} states formed by surface reduction are stabilized by lattice reconstruction (regrouping of oxygen anions around Zr^{3+} at elevated temperatures) and become more stable than Zr^{4+} states. This decreases hole recombination through Zr^{3+} defects, and therefore increases the probability for holes to react with hydrogen. In other words, surface reduction decreases the efficiency of surface recombination which, in turn, increases the efficiency of surface (both oxidation and reduction) reactions.

3.2. Photoselectivity

We noted earlier (see Section 1) that the ratio $\gamma = [e^-]/[h^+]$ is one of those key parameters that determine the selectivity of a photocatalyst. It can be readily shown that for the same state (oxidized or reduced) of the photocatalyst, this ratio scales with the ratio between the quantum yields of photoinduced reduction and oxidation of O_2 and H_2, respectively (Eq. (12)). That is, when

$$\frac{\Phi_{O_2}}{\Phi_{H_2}} = \frac{k_e[S_e][e_S{}^-]}{k_h[S_h][h_S{}^+]} = \text{const.}\,\gamma \tag{12}$$

the photoreduction of oxygen predominates on the surface over the photooxidation of hydrogen, the ratio Φ_{O_2}/Φ_{H_2} should then scale with $\gamma = [e^-]/[h^+]$. However, when the photooxidation of hydrogen on the surface predominates over the photoreduction of oxygen, then the ratio Φ_{H_2}/Φ_{O_2} should scale with $1/\gamma = [h^+]/[e^-]$ (Eq. (13)):

$$\frac{\Phi_{H_2}}{\Phi_{O_2}} = \frac{k_h[S_h][h_S{}^+]}{k_e[S_e][e_S{}^-]} = \frac{1}{\text{const.}\,\gamma} \tag{13}$$

where k_e and k_h are the rate constants for electron and hole trapping by the corresponding surface-active sites S_e and S_h, respectively. Consequently, the spectral variation of the ratio of the quantum yields corresponds to the spectral variation of the ratio between electron and hole concentrations at the surface, which in turn is a cause for the spectral changes in selectivity of the metal-oxide photocatalyst. Fig. 4 for the oxidized state of ZrO_2 and Fig. 5 for the reduced state of ZrO_2 display the spectral dependencies of the ratio of quantum yields of photoreduction of O_2 and photooxidation of H_2, Φ_{O_2}/Φ_{H_2}, which scales with γ. The inverse ratio Φ_{H_2}/Φ_{O_2} scales with $1/\gamma$.

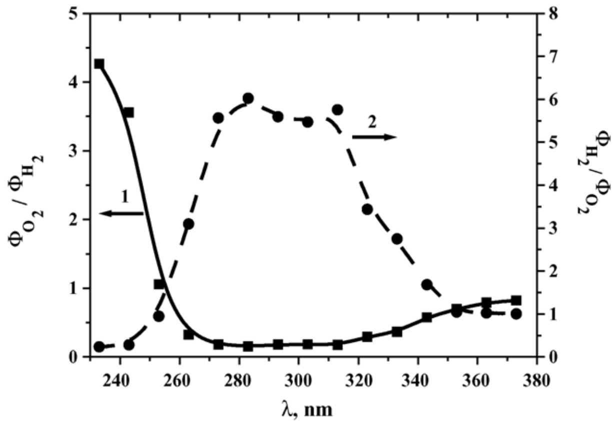

Fig. 4. Spectrally dependent ratios between quantum yields of the photoinduced reduction of oxygen and oxidation of hydrogen on oxidized zirconia particles: (1) Φ_{O_2}/Φ_{H_2} ratio which scales with γ, and (2) Φ_{H_2}/Φ_{O_2} ratio which scales with $1/\gamma$.

The reported spectral dependencies of the ratios of quantum yields indicate that photoexcitation of zirconia in the intrinsic spectral region ($\lambda < 260$ nm) shifts the selectivity toward the reduction pathway with the most dramatic changes seen at the fundamental absorption edge, as predicted by the models [12,13]. Indeed, these models inferred that the spectral variation of selectivity originates from differences in the lifetimes and mobilities of electrons and holes, and from changes in the surface potential which favors drift of one type of charge carrier (e.g. electrons) from the bulk to the surface and prevents the drift of the other type (holes) of carriers. By contrast, in the extrinsic spectral region, the spectral variation of photoexcitation should cause an increase in the efficiency of the photooxidation pathway with maximal selectivity toward oxidation products in the wavelength range 260 nm < λ < 360 nm, as evident in Figs. 4 and 5 regardless of the state of zirconia. Thus, in terms of selectivity, the behavior of zirconia as a photocatalyst is expected to depend on the spectral region of photoexcitation, which should lead to a significant difference in the composition of reaction products between the intrinsic and extrinsic spectral region of photoexcitation.

In summary then, the experimental data reported herein on the spectral dependencies of quantum yields of photoredox reactions of probe molecules (oxygen and hydrogen) have

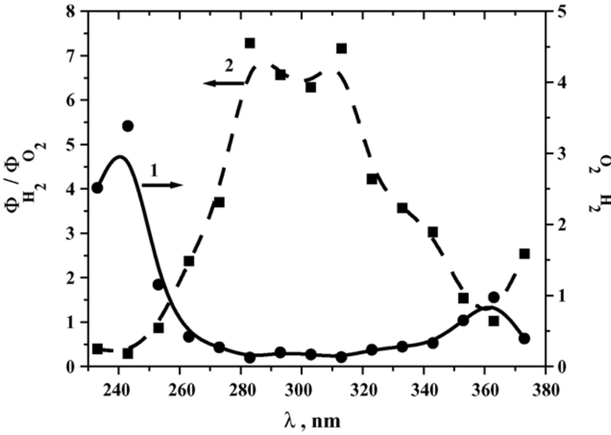

Fig. 5. Spectrally dependent ratios between quantum yields of the photoinduced reduction of oxygen and photoinduced oxidation of hydrogen on reduced zirconia particles: (1) Φ_{O_2}/Φ_{H_2} ratio which scales with γ, and (2) Φ_{H_2}/Φ_{O_2} ratio which scales with $1/\gamma$.

provided the long sought-after spectral variations into the photoactivity and photoselectivity of metal-oxide photocatalysts in gas/solid heterogeneous systems.

Acknowledgments

We are grateful to the North Atlantic Treaty Organization, Brussels, for a Collaborative Grant (No. PDD(CP)-PST CLG-979700) between our respective laboratories at Concordia University in Montreal (Canada) and at the University of St. Petersburg (Russia). Studies carried out at the Università di Pavia are supported from a grant from the Ministero dell'Istruzione, dell'Università e della Ricerca (MIUR, Roma, Italia to N.S.).

References

[1] A.V. Emeline, A.V. Panasuk, N.V. Sheremetyeva, N. Serpone, J. Phys. Chem. B 109 (2005) 2785.
[2] L. Jing, B. Xin, F. Yuan, B. Wang, K. Shi, W. Cai, H. Fu, Appl. Catal. A: Gen. 275 (2004) 49.
[3] A. Nagasaki, H. Sakai, M. Shimazaki, T. Kakihara, T. Kono, N. Momozawa, M. Abe, Shikizai Kyokaishi 72 (1999) 665.
[4] I. Alxneit, M. Corboz, J. Phys. IV: Proc. Pr3 9 (1999) 295.
[5] M.A. Blesa, Proceedings of the 224th ACS National Meeting, Boston, MA, August 18–22, 2002 (Abstracts of Papers).
[6] Z. Czarni, J. Oszczudlowski, React. Kinet. Catal. Lett. 25 (1984) 213.
[7] G.A. El-Shokaby, N.S. Petro, Surf. Technol. 9 (1979) 31.
[8] N. Serpone, A. Salinaro, A.V. Emeline, V.K. Ryabchuk, J. Photochem. Photobiol. A: Chem. 130 (2000) 83.
[9] D. Meisel, in: E. Pelizzetti, M. Schiavello (Eds.), Photochemical Conversion and Storage of Solar Energy, Kluwer, Dordrecht, The Netherlands, 1991, pp. 15–26.
[10] F.A. Houle, J. Vac. Sci. Technol. B: Microelectr. Nanom. Struct. 7 (1989) 1149.
[11] N. Serpone, A.V. Emeline, Int. J. Photoenergy 4 (2002) 91.
[12] A.V. Emeline, V.K. Ryabchuk, N. Serpone, J. Phys. Chem. B 103 (1999) 1316.
[13] A.V. Emeline, A.V. Frolov, V.K. Ryabchuk, N. Serpone, J. Phys. Chem. B 107 (2003) 7109.
[14] A.V. Emeline, N. Serpone, J. Phys. Chem. B 106 (2002) 12221.
[15] L.L. Basov, Yu.P. Solonitzyn, Patent No. 387730 (1973), Bulletin of the Invention Committee of the USSR, No. 28.
[16] A.V. Emeline, G.N. Kuzmin, D. Purevdorj, V.K. Ryabchuk, N. Serpone, J. Phys. Chem. B 104 (2000) 2989.
[17] K. Endo, M. Ono, H. Kawahura, K. Obara, Patent JP 07272646 A2 19951020 Heisei (1995), Jpn. Kokai Tokkyo Koho.
[18] R. Field, S. Hang, T. Arnot, J. Membr. Sci. 86 (1994) 291.
[19] Y. Murai, K. Omura, Patent JP 60222759 A2 19851107 Showa (1985), Jpn. Kokai Tokkyo Koho.
[20] T. Yamaguchi, Sekiyu Gakkaishi 36 (1993) 250.
[21] H.N. Bansal, Can. Metall. Quart. 15 (1976) 183.
[22] A.J. Raigrodski, J. Prosthet. Dent. 92 (2004) 557.
[23] R. Hartung, R. Schroeder, H.H. Moebius, Z. Physik. Chem. (Leipzig) 262 (1981) 961.
[24] Y. Kubota, M. Nishimatsu, T. Ide, K. Noguchi, K. Kobayashi, Patent DE 3334305 A1 19840419 (1984), Ger. Offen.
[25] Ch.B. Luschik, A.Ch. Luschik, Decay of Electronic Excitation with Formation of Defects in Solids, Nauka, Novosibirsk, Russia, 1989 (in Russian).
[26] V.N. Strekalovsky, Yu.M. Polejaev, S.V. Palguev, Oxides with Extrinsic Disorder, Nauka, Moscow, Russia, 1987.
[27] M.M. Mikhailov, N.Y. Kuznetsov, Neorgan. Mater. 24 (1988) 656.
[28] M.M. Mikhailov, M.I. Dvoretsky, N.Y. Kuznetsov, Neorgan. Mater. 20 (1984) 449.
[29] D.E. Harrison, N.T. Melamed, E.G. Subbarao, J. Electrochem. Soc. 110 (1963) 23.
[30] C. Bettinali, G. Ferraresso, J.W. Manconi, J. Chem. Phys. 50 (1969) 3957.
[31] C. Bettinali, G. Ferraresso, J. Am. Ceram. Soc. 53 (1970) 495.
[32] P. Jacconi, D. Lapros, R. Caura, Phys. Status Solidi A 50 (1978) 275.
[33] G.V. Burukina, PhD Thesis, Leningrad State University, Leningrad, Soviet Union, 1990.
[34] I.M. Prudnikov, Personal Communication to V.K. Ryabchuk, 1998.
[35] G.V. Gezalov, A.A. Garibov, R.D. Kasumov, Soviet Khimia Visokich Energii 29 (1990) 472.
[36] A.V. Emeline, G.V. Kataeva, V.K. Ryabchuk, N. Serpone, J. Phys. Chem. B 103 (1999) 9190.
[37] A.V. Emeline, G.V. Kataeva, A.S. Litke, A.V. Rudakova, V.K. Ryabchuk, N. Serpone, Langmuir 14 (1998) 5011.
[38] D.L. Doering, K.H. Siek, P. Xiong-Skiba, D.L. Carroll, Mater. Res. Soc. Symp. Proc. 316 (1994) 93.
[39] A.S. Foster, V.B. Sulimov, F. Lopez Gejo, A.L. Shluger, R.M. Nieminen, J. Non-Crystal. Solids 303 (2002) 101.
[40] V.F. Anufrienko, E.G. Avvakumov, N.T. Vasenin, S.V. Vosel, Khim. Fiz. 22 (2003) 25.
[41] J.-M. Costantini, F. Beuneu, D. Gourier, C. Trautmann, G. Calas, M. Toulemonde, J. Phys. Cond. Matter 16 (2004) 3957.
[42] G.V. Burukina, L.L. Basov, V.K. Ryabchuk, Vestnik SPBU Ser. 4 Fiz. Khim. (1993) 8.
[43] G.V. Burukina, L.L. Basov, V.K. Ryabchuk, Vestnik SPBU Ser. 4 Fiz. Khim. (1990) 32.
[44] G.V. Kataeva, A.V. Emeline, V.K. Ryabchuk, Vestnik SPBU Ser. 4 Fiz. Khim. (2003) 13.
[45] A.S. Foster, V.B. Sulimov, F. Lopez Gejo, A.L. Shluger, R.M. Nieminen, Phys. Rev. B: Cond. Matter Mater. Phys. 64 (2001) 224108/1.
[46] V.I. Aleksandrov, S.Kh. Batygov, M.A. Vishnyakova, Yu.K. Kalabukhova, S.V. Lavrishchev, E.E. Lomonova, V.A. Myzina, V.V. Osiko, Fiz. Tverdogo Tela (SPBU) 26 (1984) 1313.
[47] L.L. Basov, G.N. Kuzmin, I.M. Prudnikov, Yu.P. Solonitzyn, Usp. Photoniki. 6 (1977) 82.
[48] V.K. Ryabchuk, G.V. Burukina, Sov. J. Phys. Chem. 65 (1991) 1621.
[49] O. Kotova, PhD Thesis, Leningrad State University, Leningrad, Soviet Union, 1986.
[50] P. Pichat, J.-M. Herrman, J. Disdier, M.-N. Mozzanega, J. Phys. Chem. 83 (1979) 3122.
[51] G.V. Burukina, G.E. Vitkovsky, V.K. Ryabchuk, Vestnik SPBU Ser. 4 Fiz. Khim. (1990) 92.
[52] G.V. Burukina, PhD Thesis, Leningrad State University, Leningrad, Soviet Union, 1990.
[53] A.V. Emeline, A.V. Rudakova, V.K. Ryabchuk, N. Serpone, J. Phys. Chem. B 102 (1998) 10906.
[54] S.A. Polikhova, N.S. Andreev, S.V. Emeline, V.K. Ryabchuk, N. Serpone, J. Phys. Chem. B 108 (2004) 2354.
[55] S.-C. Moon, T. Hieida, H. Yamashita, M. Anpo, Chem. Lett. (1995) 447.
[56] S.-C. Moon, M. Fujino, H. Yamashita, M. Anpo, J. Phys. Chem. B 101 (1997) 369.
[57] C. Morterra, E. Giamello, L. Orio, M. Volante, J. Phys. Chem. 94 (1990) 3111.
[58] H. Liu, L. Feng, X. Zhang, Q. Xue, J. Phys. Chem. 99 (1995) 332.
[59] J. Crawford, Semicond. Insul. 5 (1983) 599.

[60] M.A. Monge, R. Gonzales, J.E. Munoz-Santiuste, R. Pareja, Y. Chen, E.A. Kotomin, A.I. Popov, Nucl. Instrum. Methods Phys. Res. B 166–167 (2000) 220.
[61] Q. Zhao, X. Wang, T. Cai, Appl. Surf. Sci. 225 (2004) 7.
[62] X.-P. Wang, Q. Zhao, T.-X. Cai, Huaxue Xuebao 60 (2002) 622.
[63] X.-P. Wang, Q. Zhao, Q.-S. Lin, T.-X. Cai, Gaodeng Xuexiao Huaxue Xuebao 23 (2002) 1343.
[64] W. Li, L.B. Feng, Y.Q. Yin, Chin. Chem. Lett. 7 (1996) 269.